

Dark matter phenomenology of high speed galaxy cluster collisions

Yuriy Mishchenko¹ and Chueng-Ryong Ji²

¹*Department of Computer-Software Engineering, Toros University, Mersin 33140, TURKEY*

²*Department of Physics, North Carolina State University, Raleigh NC 27695-8202, USA*

We perform a computational survey of possible post-collision mass distributions in high-speed galaxy cluster collisions in the presence of weakly self-interacting dark matter. We show that astrophysically weak self-interactions of dark matter may impart subtle yet measurable structures to the distribution of mass in high-speed collision galaxy clusters without significantly disrupting the colliding galaxy clusters or their dark matter halos. Interesting structures appear in the projected mass density maps of collision galaxy clusters as dark matter concentrations at large scattering angles and the distances from the collision center commensurate with that of the outgoing galaxy groups. Convincing observation of such structures would be a clear indication of the self-interacting nature of dark matter, as purely gravitational effects in high-speed galaxy cluster collisions are observed to produce material ejecta only in the forward and the backward cones around the collision axis. Our simulations indicate that as much as 20% of the total collision cluster mass may be deposited to produce such structures without noticeably disrupting the participating galaxy clusters or their dark matter halos. Our findings appear to explain the ring-like dark matter feature recently observed in long-range reconstructions of the mass density profile of the collision galaxy cluster CL0024+017. The size of this feature implies an estimate for the dark matter self-interaction strength of $\sigma_{DM}/m_{DM} \approx 0.1 \text{ cm}^2/g$.

I. INTRODUCTION

Dark matter and dark energy, comprising together 95% of the energy budget in the Universe, remain among the biggest unsolved mysteries of modern physics. Dark matter has been described conventionally using the Cold Dark Matter (Lambda-CDM) model, where the primary candidate for the dark matter is an extremely massive ($m_{DM} \approx 10 - 1000 \text{ GeV}$) particle interacting exclusively via the weak interaction - the so-called Weakly Interacting Massive Particle or WIMP [1, 2]. In recent years, however, observations began to suggest that dark matter can be interacting with the cross-sections large enough to influence the formation of small cosmological structures [3–11]. Recent works had put forth the models with interacting dark matter including the mirror dark matter [12], the flavor-oscillating dark matter [13], the strongly interacting dark matter [14, 15], etc.

Recently, the observations of colliding galaxy clusters provided a unique opportunity for gaining additional insight about the properties of dark matter experimentally [16–19]. These collisions, comprised of two or more galaxy clusters experiencing a high-speed central or near-central passage through each other and observed shortly after that, are a natural source of high-energy collisions of dark matter particles and can offer new clues about the microscopic properties of dark matter [16–39]. Bullet-type galaxy cluster collisions are such collisions that involve a smaller galaxy cluster, sometimes referred to as “bullet”, falling onto and passing with a high relative velocity through a much larger galaxy cluster. In several cases, we have observed a bullet-type galaxy cluster collision shortly after the passage of the bullet cluster through the main galaxy cluster [20, 22]. Those observations evinced that the galaxy groups in the bullet-type galaxy cluster collisions exhibit a collisionless behavior, that is, pass through each other freely and without significant non-gravitational interactions. On the other hand, the gas components of the colliding galaxy clusters—the inter-cluster medium or ICM—exhibit a drastically different behavior with significant ram friction, super-sonic bow-shocks, and strong heating accompanied and X-ray emission [16, 17, 23, 28]. Subsequent reconstructions of the mass distribution in some of such bullet-type collision galaxy clusters using strong and weak gravitational lensing revealed that the dark matter in these collisions is co-localized with the collisionless galaxy groups but not with the collisional ICM gas [16–39]. This co-localization allowed to conclude that the material comprising the dark matter halos behaves in a collisionless manner, much like the galaxy groups rather than the inter-cluster medium. More precise arguments such as the preservation of the dark matter halos and the light-to-dark ratios as well as the rough coincidence of the centroids of the dark matter halos with that of the galaxy groups allowed to put a constraint on the cross-section of the interactions of the dark matter particles comprising the galaxy clusters’ dark matter halos at $\sigma_{DM}/m_{DM} < 1 \text{ cm}^2 g^{-1}$ [16, 20, 21, 27, 30, 34, 40].

In this work, we perform a comprehensive computational survey of possible mass distributions in high-speed collision galaxy clusters in relation to possible presence of weakly self-interacting dark matter. In the past, several computational studies had focused on the simulations of actually observed collision galaxy clusters and deducing the bounds on the interaction cross-section of dark matter from such simulations [24, 27, 29, 30, 39, 41, 42]. Here, we aim to perform a survey of different possibilities that can be realized in high-speed galaxy cluster collisions under a variety of conditions. Our particular emphasis is to look for the effects introduced by small but nonzero dark matter self-

interactions that impact on the post-collision mass distributions. Our numerical simulations provide a more in-depth insight on the features of the mass distributions in the observed collision galaxy clusters. For instance, we find that more strongly interacting dark matter particles with $\sigma_{DM}/m_{DM} \approx 1 \text{ cm}^2 g^{-1}$ cause severe disruptions of the dark matter halos of the colliding galaxy clusters leading typically to their complete destruction and rapid merger. This is in contrast to the prior emphasis on minor effects such as the lag of the halos' centroids behind that of the galaxy groups [16, 20, 21, 34, 40]. We also find that a range of weaker interaction cross-sections $\sigma_{DM}/m_{DM} \approx 0.1 \text{ cm}^2 g^{-1}$ can produce detectable albeit weak features in the mass distribution of a collision galaxy cluster. Such features include radial dark matter ejecta produced by single-scattering of dark matter particles during the time of the galaxy clusters' passage through each other. These can appear in the projected mass density maps of collided galaxy clusters as weak off-axial concentrations of dark matter at large scattering angles and the distances from the collision center comparable to that of the outgoing galaxy groups. Interestingly, structures resembling such features can be observed in the reconstructions of the projected mass density maps of many collision galaxy clusters available in the literature [28, 34, 36, 37]. In the collision of galaxy clusters seen along the line of the collision, such features can appear as weak rings of dark matter that can be observed around the central mass peak. Such a feature had been recently reported in a long-range reconstruction of the mass distribution in the galaxy cluster CL0024+17 [26].

The rest of this paper is presented as follows. In Section II, we discuss the methodological details of our simulations. In Section III, we survey different types of possible post-collision mass distributions in colliding galaxy clusters with respect to parameters such as collision speed, mass, dark matter interactions' strength, etc. The summary and conclusions follow in Section IV.

II. METHODOLOGY

For the purpose of simulating the galaxy cluster collisions in the presence of different weak dark matter (DM) self-interactions, we implement the Particle Mesh algorithm in Matlab that can be used to solve the problem of many body gravitational dynamics. Specifically, in the Particle Mesh algorithm, the gravitational evolution of a continuous spatial distribution of mass $\rho(\vec{x}, t)$ is modeled using a collection of N particles $\vec{r}_i(t)$, $i = 1 \dots N$, distributed according to $\rho(\vec{x}, t)$. As the particles move in the common gravitational potential $\Phi(\vec{x}, t)$, we calculate $\Phi(\vec{x}, t)$ approximating $\rho(\vec{x}, t)$ on a 3D grid \mathcal{G} by counting the number of the particles in each grid cell $\vec{x}_{\mathcal{G}}$ in \mathcal{G} , $n(\vec{x}_{\mathcal{G}}, t)$, and then solve the Poisson equation,

$$\nabla^2 \Phi(\vec{x}, t) = 4\pi G n(\vec{x}, t), \quad (1)$$

where G is the gravitational constant. A particularly advantageous method for obtaining the solutions of Eq. (1) on \mathcal{G} is to use the Fourier transform, $\tilde{\Phi}(\vec{k}, t) = \int d\vec{x} (2\pi)^{-3/2} e^{-i\vec{k} \cdot \vec{x}} \Phi(\vec{x}, t)$, and make Eq. (1) equivalent to a simple algebraic equation,

$$\tilde{\Phi}(\vec{k}, t) = -4\pi G \frac{\tilde{n}(\vec{k}, t)}{\vec{k}^2}, \quad (2)$$

wrapped by two discrete fast Fourier transforms for $n(\vec{x}, t) \rightarrow \tilde{n}(\vec{k}, t)$ and $\tilde{\Phi}(\vec{k}, t) \rightarrow \Phi(\vec{x}, t)$. Once $\Phi(\vec{x}, t)$ is calculated, both the speed and the position of all particles are updated according to the usual Newtonian dynamics. The simulation is advanced in time using an adaptive time step Δt , which is defined by restricting the maximum change in the speed and the position of simulation particles and typically varied between 0.1 My and 10 My.

In order to model non-gravitational interactions in the dark matter halos of colliding galaxy clusters, two particles in the simulation were assumed to be able to scatter on each other elastically with the probability

$$P = \alpha V_{rel} \Delta t, \quad (3)$$

if and only if they occupied the same grid cell at the same time. Here, $V_{rel} = |\vec{v}_1 - \vec{v}_2|$ is the relative speed of the particles, Δt is the simulation time step, and α is an effective parameter that set the strength of the dark matter self-interactions. The parameter α was chosen in the simulations a-posteriori, so as to achieve a given fixed fraction of the dark matter particles scattered during the galaxy clusters collision. To simulate elastic scatterings of dark matter particles, the Center-of-Mass velocity, \vec{V}_{CM} , for any two simulation particles that scattered was computed and the initial velocities of the scattered simulation particles in their center-of-mass frame, $\vec{v}_{1;CM}$ and $\vec{v}_{2;CM}$, were found before the scattering. As required by the conservation of energy and momentum in elastic collisions of identical particles, the magnitudes of $\vec{v}_{1;CM}$ and $\vec{v}_{2;CM}$ were preserved after the scattering while the directions of the final velocities, $\vec{v}'_{1;CM}$ and $\vec{v}'_{2;CM}$, were randomly changed on a unit sphere. The post-scattering velocities of the simulation particles were set as $\vec{v}'_1 = \vec{V}_{CM} + \vec{v}'_{1;CM}$ and $\vec{v}'_2 = \vec{V}_{CM} + \vec{v}'_{2;CM}$.

All simulations were performed with $N = 2 \cdot 10^5$ particles simulated on a cubic lattice of $D = 64 \cdot 10^6$ points, modeling a region of space 6 Mpc on each side. For the simulations, the super-computing facilities in the National Energy Research Scientific Computing Center (NERSC) were used. All simulations were performed using only dark matter halos and ignoring the ICM and the visible galaxies contributions. All simulations were performed for the total period of 1.5 Gy to 3 Gy, typically spanning a single passage of the dark matter halos through each other in a collision. All simulations were initialized with two dark matter halos represented by particle clouds at large separations from each other $d \approx 2 \text{ Mpc}$, moving towards each other with relative velocities ranging from 500 km/s to 3000 km/s. The initial particles in the clouds were generated according to the equilibrium mass profile obtained by gravitationally equilibrating the particles inside the halos in isolation for at least 10 Gy. In the case of the simulations of off-centered galaxy cluster collisions, the centers of the initial particle clouds were also shifted with respect to each other in the direction perpendicular to the axis connecting their centers, realizing the impact parameter equal to the core radius of the larger of the colliding clusters. In this way, the effect on the post-collision mass distribution was maximized, since much larger impact parameters would result in the clusters mostly missing each other's dense cores and much smaller impact parameters would result in post-collision mass distributions similar to that of a fully central collision. In the case of the simulations of symmetric galaxy cluster collisions, the colliding dark matter halos were initialized in equal configuration taking each of the galaxy cluster with mass $M = 2.5 \cdot 10^{14} M_\odot$. In the simulations of asymmetric collisions, the two halos were initialized in the ratio of masses 5:1, with the total mass $M_{tot} = 5 \cdot 10^{14} M_\odot$. This choice was made to achieve the simulation scenarios similar to the classical example of the high-speed galaxy cluster collisions — the Bullet cluster 1E 0657-56 [18, 22, 31].

Different galaxy cluster collision scenarios were simulated by varying the following parameters in the above settings: the initial (at infinity) infall speed of the colliding galaxy clusters, the impact parameter of the collision, the similarity of the colliding clusters' sizes, and the effective parameter a to set the strength of the DM-DM particle scattering. The total mass of the collision was not varied in the simulations because it can be reduced from the dynamic equations, $\frac{d\vec{v}(\vec{x}, t)}{dt} = -G\nabla \int d^3y \frac{\rho(\vec{y}, t)}{|\vec{x} - \vec{y}|}$, by suitably re-scaling the distances $\vec{x}' = (M_{tot}/M_0)^{1/3} \vec{x}$, where M_0 is a certain standard mass scale. Thus, in all simulations the total collision mass $M_{tot} = 5 \cdot 10^{14} M_\odot$ was maintained.

III. RESULTS

A. The phenomenology of high-speed galaxy cluster collisions in CDM model

We first study the phenomenology of high-speed galaxy cluster collisions in CDM, that is, when the gravity is the only force affecting the dynamics of the DM halos. In this case, possible phenomenologies of the collision are controlled by a single parameter defined by the ratio of the kinetic energy with respect to the mutual gravitational energy of the colliding clusters, $k = |E_{kinetic}/E_{mutual\ gravity}|$. This ratio defines the relative importance of kinetic versus gravitational effects during the collision. This definition depends on the point at which $E_{kinetic}$ and $E_{mutual\ gravity}$ are calculated. For concreteness, we set k using the kinetic energy and the mutual gravitational energy of the galaxy clusters at the point of closest approach.

The conservation of energy implies that k is related to the total energy of the colliding galaxy clusters E and their gravitational energy U at the point of closest approach (omitting the gravitational self-energy of the individual galaxy clusters) as $k = 1 + E/|U|$. Thus, we can distinguish three essentially different collision regimes: fast collisions with $E > 0$ and $k > 1$, free-fall collisions with $E = 0$ and $k = 1$, and slow collisions with $E < 0$ and $k < 1$. In fast collisions, the clusters fall towards each other with a finite impact velocity at infinity. In the free-fall case, the clusters fall towards each other from zero speed at infinity. The case $k < 1$ corresponds to the situations where the clusters fall towards each other from a smaller initial distance.

For fast collisions $k > 1$, our simulations indicate two separate regimes $k > 2$ and $2 > k > 1$. For very high speed collisions $k \approx 2$ and above, we observe a substantially different post-collision behavior of the collision galaxy cluster than that for $k \approx 1$. For the “high-speed” regime, the galaxy clusters tend to move as compact objects, passing through each other without significant disruptions. For $2 > k > 1$, however, we typically observe formation of significant high-speed ejecta of the material from the galaxy clusters' dark matter halos. These are formed typically as conic jets surrounding the clusters' initial velocity vector. In the projected mass distributions, these ejecta form notable “fan-out” shape around the collision axis as shown in the left panel of Fig. 1. A central bridge of slow material or central core, trailing the galaxy clusters from behind, also forms in this regime. Notably, however, the ejecta formation is always restricted to the forward and backward cones of small scattering angles. This observation is generally consistent with the properties of the differential cross-section in single-particle gravitational scattering.

For the free-fall case $k = 1$, we observe that the clusters nearly merge already on the first passage, producing a profound amount of ejecta in characteristic “butterfly” shape as shown in the central panel of Fig. 1. In even slower

collisions ($k < 1$), the clusters merge rapidly into a single cluster, generating a large amount of almost spherically symmetric material ejecta as shown in the right panel of Fig. 1.

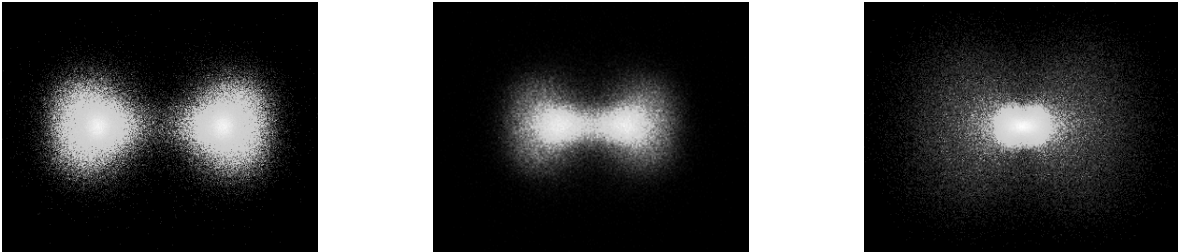


FIG. 1. Possible phenomenologies of galaxy cluster collisions in CDM model for different values of the kinetic parameter k . From left to right shown are the examples of a central symmetric fast collision $k = 1.7$, free-fall collision $k = 1$, and slow collision $k = 0.7$.

B. The phenomenology of high-speed galaxy cluster collisions in interacting DM model

In the interacting dark matter case, the phenomenology of the high-speed galaxy cluster collisions is governed primarily by two parameters: the kinetic parameter k and the effective DM-DM particle scattering strength parameter, a . The kinetic parameter k had been defined above as the ratio of the colliding galaxy clusters' total kinetic energy with respect to the total mutual gravitational energy at the time of closest approach. The effective DM-DM particle scattering strength a we define here as the fraction of the DM particles suffering at least one scattering during the galaxy clusters' first passage through each other.

The parameter a can be related to the optical depth of DM particles in DM halo $L \approx (\frac{\sigma_{DM}}{m_{DM}} \rho_{halo})^{-1}$ and the DM halo's diameter D as $a \approx D/L$. Here, σ_{DM} and m_{DM} are the interaction cross-section and the mass of DM particles and ρ_{halo} is the halo's peak mass-density. The parameter a can be thus expressed as $a \approx \frac{\sigma_{DM}}{m_{DM}} M_{\Sigma}$, where M_{Σ} is the halo's projected mass density measured in the units of [Mass/Length²].

With respect to the kinetic parameter k , we encounter three main cases of fast, free-fall, and slow collisions, as before. In this section, maintaining the focus on the high-speed collision of galaxy clusters, we primarily consider the fast galaxy clusters' collisions with $k \approx 2$ and above. With respect to the DM interaction strength parameter a , we observe three main regimes in our simulations — strongly scattering $0.5 \leq a$, weakly scattering $a \leq 0.2$, and in-between or intermediate $0.2 \leq a \leq 0.5$. The typical phenomenologies of the post-collision mass distributions in relation to these DM interaction strengths are shown in Fig. 2.

More specifically, the results shown in Fig. 2 are obtained from our simulations that modeled the collision of two galaxy clusters with the total mass of $M_{tot} = 5 \cdot 10^{14} M_{\odot}$ that was split between the two colliding galaxy clusters. While M_{tot} was split equally in the case of symmetric collisions, in the case of asymmetric bullet-type galaxy cluster collisions it was split in the ratio 5:1, as described in Section II. We varied the parameters for the strength of the DM self-interaction effects in galaxy cluster collisions as well as the collisions' speed, symmetry, and centrality. The infall of the clusters was simulated from a large distance having initially the relative velocity of 3000 km/s, achieving at the time of the passage the top velocity of 4000 km/s, and exhibiting the typical post-impact separation velocities of 2000-2500 km/s. These simulations corresponded to the value of the kinetic parameter $k = 1.7$. This scenario was chosen to be similar to the classical example of the high-speed galaxy cluster collisions—the Bullet cluster [18, 22, 31]. In the simulations of central collisions, the two galaxy clusters were simulated to move exactly towards each other having the impact parameter of zero. In off-center collisions, the collision was simulated with the impact parameter equal to the core-radius of the larger of the colliding clusters to maximize the effect of non-centrality on the post-collision mass distributions.

In Fig. 2, the mass distributions observed in the simulations are shown in the format of the table in which the columns correspond to different DM self-interaction strengths and the rows demonstrate different collision scenarios. In all simulation regimes, we observe that the increment of DM self-interaction strength results in additional dispersion introduced in the collision galaxy cluster's mass distribution, most notably including the ejecta of dark matter in equatorial plane perpendicular to the collision axis at close to 90° scattering angles.

In the case of strongly interacting dark matter, $a \approx 0.5$ and above, we observe that the mass distribution in the collision galaxy cluster becomes significantly disrupted, forming a single cloud of hot DM material shortly after the collision. However, in the case of intermediate values of $0.2 \leq a \leq 0.5$, we observe much less significant disruption of the halos while the survival of individual halos become possible.

In the most interesting case $a \leq 0.2$, we observe that the DM halos are not significantly distorted during the galaxy clusters' passage through each other, yet the features distinguishing this case from purely CDM model appear in the post-collision mass distributions. Despite the weakness of such features, their appearance is in drastic difference from the CDM case, where the gravitationally ejected material is always confined to small scattering angles in the collision's forward and backward cones, as shown in Fig. 1, and cannot be ejected at large scattering angles.

The formation of these off-axis scattering features in the case of weakly interacting dark matter can be understood by considering the process of DM particles scattering during the galaxy clusters' initial passage through the other. In the weak scattering regime $a \ll 1$, the optical depth of the DM particles is substantially greater than the diameter of the DM halos. Thus, only a small fraction of DM particles is non-gravitationally scattered during the passage. On the other hand, the particles that do scatter leave the DM halos without secondary collisions. This allows a feature in the form of a shell of dark matter expanding radially outwards from the center of the collision. The shell is formed from the scattered DM particles and includes the equatorial plane at 90° scattering angles. The precise form of this feature depends on the distribution of mass in the DM halos during the collision as well as post-collision gravitational effects. However, the presence of DM ejecta at large scattering angles is preserved even after taking into account these effects.

The distribution of the matter in the radial ejecta shell also depends on the specifics of the microscopic interactions of dark matter particles. It is reasonable to assume as a first guess that the DM-DM interactions in the conditions of a galaxy cluster collision would be elastic and short range. In such case, it can be further fathomed that the scattering cross-section of the DM particles at the relevant energy scales would be isotropic. Indeed, the low energy spin-averaged cross-sections of all short-range interactions, including the strong and the weak interactions, are isotropic. So are the solutions of all quantum-mechanical scattering problems with δ -function-like short-range potentials. If we accept this assumption, then the DM ejecta shell formed during the scattering of the DM particles in a galaxy cluster collision can be expected to be spherically symmetric. The conservation of energy and momentum further implies that the speed of scattered particles is conserved during DM-DM scattering events. Consequently, the expansion speed of the shell of the scattered material will be equal to that of the outgoing galaxy clusters. In other words, the scattered DM ejecta shell expands essentially together with the outgoing galaxy clusters. In the projected mass density maps, the DM scattering feature can be expected to appear as a shell connecting the respective galaxy groups for the collisions observed perpendicularly to the collision axis, or as a ring surrounding the central mass peak for the collisions observed parallel to the collision axis, as shown in Fig. 3.

C. Optimal detection conditions

The DM-DM interactions in weakly scattering regime $a \approx 0.1 - 0.2$ do not result in significant disruptions to the colliding galaxy clusters or their halos such as the destruction of the original DM halos, a noticeable change in halos' light-to-mass ratios, or DM halos drag. At the same time, such weakly interacting regime is capable of introducing distinctive features in the post-collision mass distributions such as dark matter structures above background at close to 90° scattering angles.

The observation of such features is complicated by their extremely low mass. For instance, at $a \approx 0.1$ at most 10% of the combined galaxy cluster mass can be contributed to the formation of the radial DM ejecta. While such features are very weak, their remote location from the collision axis as well as from most of the gravitational ejecta and hot ICM may allow the experimental observation of such features under favorable conditions. We may then ask a question "Under what conditions are the chances of detecting the radial dark matter outflows maximized in the collisions of galaxy clusters?".

To answer this question, we focus on central symmetric galaxy cluster collisions, where we expect the amount of produced DM ejecta naturally to be the greatest. We fix the DM-DM scattering strength parameter at $a \approx 10\%$, taking into account the fact that in the astrophysically observed collision galaxy clusters there appear to be no significant disruptions in the colliding galaxy clusters' halos. Under these conditions, possible observation regimes are characterized by just a handful parameters such as the galaxy clusters' total mass, collision speed, the clusters' total kinetic and gravitational energies. Not all of these are independent. In particular, the total kinetic energy in these scenarios scales linearly with the total clusters mass, M , while gravitational energy scales as M^2 . Therefore, it is possible to remove the total collision mass from the dynamics by choosing a suitable scale for the distances in the simulations, as mentioned in Sec.II. The only independent parameter is the ratio of the collision's total kinetic and gravitational energy, the kinetic parameter k .

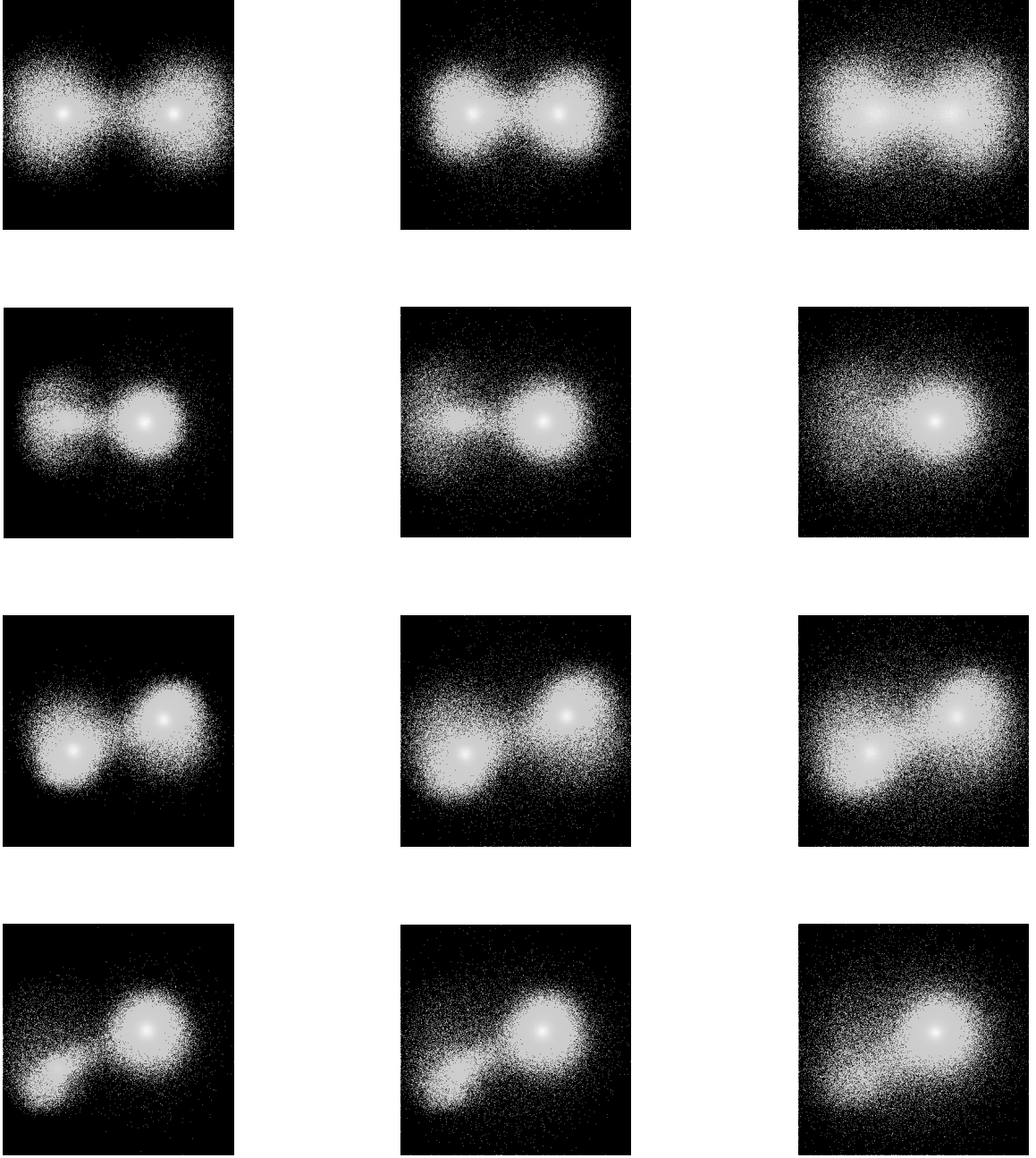


FIG. 2. The phenomenologies of possible post-collision mass configurations in galaxy cluster collisions with respect to the interaction strength of dark matter as well as the centrality and the asymmetry of the collisions. Different galaxy cluster collision scenarios illustrated are: left column - CDM model, center column - weak interacting DM model with $a = 0.1$, right column - strong interacting DM model with $a = 0.5$; 1st row - central symmetric collision, 2nd row - central asymmetric collision, 3rd row - off-center symmetric collision, 4th row - off-center asymmetric collision. The collision's kinetic parameter $k = 1.7$ in all cases.

With respect to different values of the collision's kinetic parameter k , we observe that the formation of gravitational ejecta is suppressed at higher values of k , while the ejecta produced due to the DM-DM particle scattering is unaffected by k , as shown in Fig. 4. This effect can be expected, since the gravitational ejecta are produced due to differential acceleration of different parts of the halos of the infalling galaxy clusters, which are suppressed at higher cluster speeds. At the same time, the rate of scattering of the DM particles is only increased as the relative speed of the DM

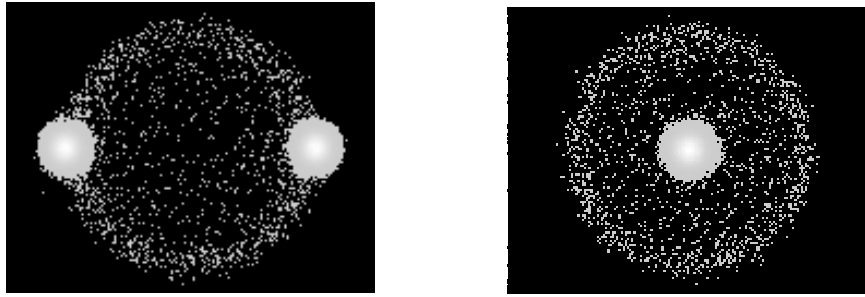


FIG. 3. The mass distribution for a weakly interacting DM model in an “ideal” case of two fast compact colliding galaxy clusters. The left panel shows the projected mass density map for a collision observed perpendicular to the collision axis, and the right panel shows such a distribution for a collision seen through the collision axis.

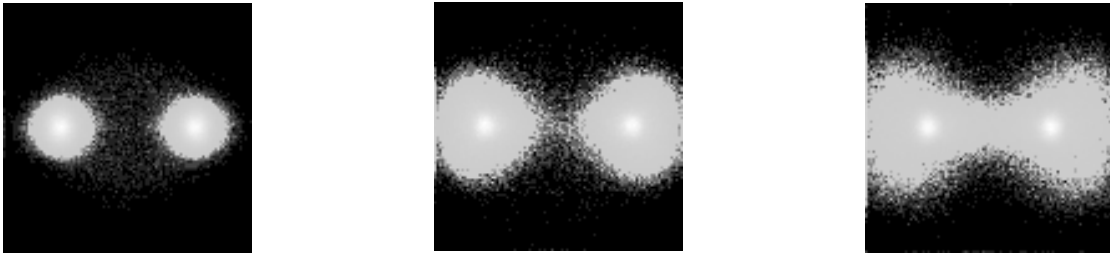


FIG. 4. The phenomenologies of galaxy cluster collisions with weakly interacting dark matter. From left to right shown are the examples of fast central symmetric collisions with $k = 4.0$, $k = 2.0$, and $k = 1.5$. The DM-DM scattering strength in all simulations is constant at $a = 0.1$. Each figure shows the view of the complete region of space in the simulation.

halos increases. Thus, the ejecta due to DM-DM scattering will appear the most distinctively in the collision galaxy clusters with very high k .

In Table I, we list the closest-approach relative collision velocities for different values of k in relation to the collision’s total mass M_{tot} . As can be seen from this table, for very heavy galaxy clusters the collision speeds required to achieve $k \approx 2 - 4$ are very high. At the same time, higher values of the collision’s kinetic parameter k can be achieved with lower collision speeds in the collisions of lighter structures. For example, for the collision masses $M \approx 10^{14}M_{\odot} - 10^{13}M_{\odot}$, the values of the kinetic parameter $k \approx 4 - 8$ can be achieved with the closest-approach speeds of 800-2500 km/s. This mass range corresponds to the collisions of compact galaxy clusters and heavy galaxy groups. Of course, this mass range also provides the worst chances for the reconstruction of the post-collision mass distributions by means of the classical approach of gravitational lensing.

As a second factor affecting the observability of the DM-DM scattering effects in galaxy cluster collisions, we consider whether the observation of such collisions in the plane of the collision or along the collision axis constitutes a more favorable condition. We observe that for the galaxy cluster collisions observed in the plane of the collision the presence of complex gravitational ejecta and ICM gas may hinder the observation of weak DM-DM scattering effects. For the collisions observed along the axis of the collision, however, the gravitational ejecta is concentrated around (or more accurately, above and below) the colliding galaxy clusters, thus, making the contribution to the projected mass density profiles at and immediately around the central mass peak. The shell of scattered DM material, then, may be seen more clearly in this case as a ring-like structure around the central mass peak in the projected mass density as exemplified in Fig. 3. Thus, the galaxy cluster collisions observed through the collision axis constitute a more favorable condition for the observation of the weak DM-DM scattering effects.

TABLE I. The closest approach relative collision speed in relation to the collision's kinetic parameter k and total collision's mass M_{tot} .

k	$10^{15} M_{\odot}$	$5 \cdot 10^{14} M_{\odot}$	$10^{14} M_{\odot}$	$5 \cdot 10^{13} M_{\odot}$	$10^{13} M_{\odot}$
1	4000 km/s	2800 km/s	1300 km/s	900 km/s	402 km/s
2	5600 km/s	4000 km/s	1800 km/s	1300 km/s	560 km/s
4	8000 km/s	5600 km/s	2500 km/s	1800 km/s	800 km/s
8	11300 km/s	8000 km/s	3600 km/s	2500 km/s	1130 km/s

IV. SUMMARY AND DISCUSSION

In this work, we studied the phenomenology of possible mass distributions in high-speed galaxy cluster collisions such as the Bullet cluster 1E 0657-56, MACSJ 0025-1222, Abell520, Abell754, etc. The phenomenology of the high-speed galaxy cluster collisions in relation to weakly interacting DM can be characterized by two main parameters — the ratio of the kinetic and gravitational energy in the collision, k , and the fraction of the particles in the DM halos that scatter via DM-DM interactions during the collision, a .

With respect to the kinetic parameter k , we observe three main regimes of the galaxy cluster collisions. For the collisions with very high speed $k > 2$, the galaxy clusters pass through each other largely undisturbed. For the collisions with a little less but still high speed $2 > k > 1$, the collision typically produces axial “fan-out” ejecta of DM material via gravitational scattering. This gravitational ejecta, however, are always confined to small scattering angles in the forward and backward cones around the clusters’ velocity vector. For slow collisions, we distinguish free-fall collisions ($k = 1$) and slow collisions ($k < 1$). In both of these, the kinetic energy of the clusters becomes insufficient to ensure their separation after the first passage through each other and a rapid merger results, producing a characteristic “butterfly” profile in the post-collision mass distribution that surrounds the merger.

With respect to the DM-DM scattering strength parameter a , we observe three main regimes. For strongly interacting DM in which over 50% of DM halos re-scatter during the initial passage of the galaxy clusters through each other, $a > 0.5$, we observe that the DM halos are rapidly destroyed in the collisions. This disruption is severe and results in the formation of a single common halo containing highly heated DM material. As such, this outcome is far beyond the limited effects restricted to the changes in light-to-mass ratio or a lag of DM halos relative to the galaxy groups, which was discussed previously in the literature. Instead, complete and rapid reorganization of the entire DM halo is observed. We don’t observe the formation of dark central cores discussed in certain papers in the literature. This can be explained by large amounts of thermal energy deposited into the DM halos under the conditions of a high-speed galaxy cluster collision.

For weakly interacting DM in which roughly 10% to 20% of DM particles suffer scattering during the collision, $a \approx 0.1 - 0.2$, the formation of radial DM shells of singly scattered DM particles is observed. This feature can be understood by considering the scattering of DM particles in the galaxy clusters’ DM halos during the initial passage of the clusters through each other, under the conditions of DM particles’ optical depth being greater than the size of the DM halos. Such feature appears in the projected mass density maps reconstructed in gravitational lensing approach as DM structures at large scattering angles and large distances from the collision center. This makes them distinct from the gravitational ejecta in CDM model and ICM. Such structures move away from the collision center together with the outgoing galaxy groups and should appear in the projected mass density maps in a very specific configurations. This may allow their identification in the mass maps of actually observed collision galaxy clusters.

The interaction regime $0.2 \leq a \leq 0.5$ features noticeable DM halos disruption as well as the formation of radial DM outflows and assumes an intermediate place between the strongly interacting and weakly interacting DM regimes.

Previous analyses of the properties of DM particles for given observed collision galaxy clusters typically focused on the implications of the absence of major disruption effects in the collided galaxy clusters’ halos [16, 20, 21, 27, 30, 34, 40]. The effects considered from this perspective typically included a change in the overall mass-to-light ratio of the DM halos of collided galaxy clusters or the drag and the lag of the DM halos relative to the corresponding galaxy groups. In the present analysis, we performed a comprehensive study of possible galaxy cluster collision scenarios to find that weak DM interactions may impart subtle yet noticeable features in the distribution of mass outside the main halos of the smashed galaxy clusters. We find that the ejecta of DM material formed via weak DM-DM particle scattering can result in DM structures appearing in the projected mass density maps at very large scattering angles as well as large distances from the collision center. Such structures are forbidden in purely gravitational collision scenarios, whereas the ejecta produced by purely gravitational effects are concentrated in high speed collisions only in the forward and the backward cones around the collision axis. Weak DM-DM scattering structures appear as roughly spherical shells of DM material encircling the collision galaxy clusters in a rough alignment with the outgoing galaxy groups, which may admit up to 10% to 20% of the total galaxy cluster mass without a noticeable disruption to the

main DM halos.

The remote location of the weak DM-DM scattering structures either from the outgoing galaxy clusters or central hot ICM gives hope that such structures can be observed under favorable astrophysical conditions. Such structures can be recognized in the projected mass density maps of collision galaxy clusters as the concentrations of dark matter at close to 90° scattering angles and the distances from the collision center comparable to that of the outgoing galaxy groups, if the collision is observed in its plain. In the collisions observed through the collision axis, such structures would appear as ring-like DM features surrounding the central mass peak. Such structures can be observed most clearly in the collisions with high values of the kinetic parameter k . Such scenarios may be realized in the high-speed collisions of small galaxy clusters or heavy galaxy groups. The best observation conditions are presented by the collisions observed along their collision axis.

The survey of the literature on the weak and strong gravitational lensing reconstructions of the mass density maps in the currently known collision galaxy clusters shows quite interestingly that many of these maps indeed contain DM features similar to the structures described above. In particular, projected mass distributions of the collision galaxy clusters A754 and A520 both show off-axial concentrations of DM at the scattering angles close to 90° and at the same distance from the collision center as that of the outgoing galaxy groups [28, 37]. Weak and strong lensing reconstructions of the projected mass density in the classical example of the Bullet cluster also show off-axial dark mass distribution occupying a roughly spherical area between the outgoing galaxy groups. The diameter of that spherical distribution commensurates with the separation between the galaxy groups [22].

More interestingly, the recent long-range reconstructions of the projected mass density profile in the strongly lensing galaxy cluster CL0024+017, now figured as a collision galaxy cluster seen through the axis of the collision, show a large ring-like DM structure surrounding the central mass peak [26]. The corresponding structure is illustrated in Fig. 7 and Fig. 10 of Ref. [26]. Our results suggest that this structure may be indeed the remnants of the weak DM ejecta created by DM-DM particle scattering during the galaxy clusters' initial collision. The size of the structure estimated from the radial mass density profile in Fig. 10 of Ref. [26] allows us to place an estimate on the total mass contained in that structure at approximately 10% of the total cluster's mass, respectively implying the DM self-interaction strength of the order of $\sigma_{DM}/m_{DM} \approx 0.1 \text{ cm}^2/g$.

ACKNOWLEDGMENTS

This work was supported in part by the American Physical Society International Travel Grant Award Program (APS ITGAP) and in part by the US Department of Energy under Contract NO. DE-FG02-03ER41260. This research also used the resources of the National Energy Research Scientific Computing Center, which is supported by the Office of Science of the U.S. Department of Energy under Contract No. DE-AC02-05CH11231. YM also would like to acknowledge the support from the Bilim Akademisi—The Science Academy (Istanbul, Turkey) young investigator award under the BAGEP program.

-
- [1] G. Bertone, D. Hooper, and S. J. Physics Reports **405**, 279 (2005).
 - [2] L. Baudis, Nuclear Physics B **235-236**, 405 (2013).
 - [3] M. R. Buckley and P. J. Fox, Physical Review D **81**, 083522 (2010).
 - [4] R. Cyburt, B. Fields, V. Pavlidou, and B. Wandelt, Physical Review D **65**, 123503 (2002), arXiv:0203240 [arXiv:astro-ph].
 - [5] C. S. Kochanek and M. White, The Astrophysical Journal **534**, 514 (2000).
 - [6] A. Pontzen and F. Governato, Nature **506**, 171 (2014).
 - [7] B. D. Wandelt, R. Dave, C. R. Farrar, P. C. McGuire, D. N. Spergel, and P. J. Steinhardt, arXiv:astro-ph/0006344 (2000).
 - [8] N. Yoshida, V. Springel, and S. D. M. White, The Astrophysical Journal **535**, L103 (2000).
 - [9] R. Massey, L. Williams, R. Smit, M. Swinbank, T. Kitching, and D. Harvey, Mon **449**, 3393 (2015).
 - [10] Y. Mishchenko and C.-R. Ji, Physical Review D **68**, 063503 (2003).
 - [11] L. L. R. Williams and P. Saha, Monthly Notices of the Royal Astronomical Society **415**, 448 (2011).
 - [12] R. Foot, Physics Letters B **728**, 45 (2014).
 - [13] M. V. Medvedev, Physical Review Letters **113**, 071303 (2014).
 - [14] Y. Hochberg, E. Kuflik, T. Volansky, and J. G. Wacker, Physical Review Letters **113**, 171301 (2014).
 - [15] D. M. Jacobs, G. D. Starkman, and B. W. Lynn, arXiv:1410.2236 (2014).
 - [16] M. Bradač, Nuclear Physics B - Proceedings Supplements **194**, 17 (2009).
 - [17] M. Bradac, S. W. Allen, T. Treu, H. Ebeling, R. Massey, R. G. Morris, A. von der Linden, and D. Applegate, The Astrophysical Journal **687**, 959 (2008).
 - [18] D. Clowe, M. Bradac, A. H. Gonzalez, M. Markevitch, S. W. Randall, C. Jones, and D. Zaritsky, The Astrophysical Journal Letters **648**, L109 (2006), arXiv:0608407v1 [arXiv:astro-ph].

- [19] D. Clowe, S. Randall, and M. Markevitch, Nuclear Physics B - Proceedings Supplements **173**, 28 (2007).
- [20] D. Clowe, A. Gonzalez, and M. Markevitch, arXiv:astro-ph/0312273, 1 (2003), arXiv:0312273v1 [arXiv:astro-ph].
- [21] M. Markevitch, A. H. Gonzalez, D. Clowe, A. Vikhlinin, W. Forman, C. Jones, S. Murray, and W. Tucker, The Astrophysical Journal **606**, 819 (2004), arXiv:0309303v2 [arXiv:astro-ph].
- [22] M. Bradac, D. Clowe, A. H. Gonzalez, P. Marshall, W. Forman, C. Jones, M. Markevitch, S. Randall, T. Schrabback, and D. Zaritsky, The Astrophysical Journal **652**, 937 (2006).
- [23] G. W. Angus, B. Famaey, and H. S. Zhao, Monthly Notices of the Royal Astronomical Society **371**, 138 (2006).
- [24] V. Springel and G. R. Farrar, Monthly Notices of the Royal Astronomical Society **380**, 911 (2007).
- [25] A. Mahdavi, H. Hoekstra, A. Babul, D. D. Balam, and P. L. Capak, The Astrophysical Journal **668**, 806 (2007).
- [26] M. J. Jee, H. C. Ford, G. D. Illingworth, R. L. White, T. J. Broadhurst, D. A. Coe, G. R. Meurer, A. van der Wel, N. Benitez, J. P. Blakeslee, R. J. Bouwens, L. D. Bradley, R. Demarco, N. L. Homeier, A. R. Martel, and S. Mei, The Astrophysical Journal **661**, 728 (2007).
- [27] S. W. Randall, M. Markevitch, D. Clowe, A. H. Gonzalez, and M. Bradac, The Astrophysical Journal **679**, 1173 (2008).
- [28] N. Okabe and K. Umetsu, arXiv:astro-ph/0702649, 1 (2008), arXiv:0702649v4 [arXiv:astro-ph].
- [29] A. Nusser, Monthly Notices of the Royal Astronomical Society **384**, 343 (2008).
- [30] C. Mastropietro and A. Burkert, Monthly Notices of the Royal Astronomical Society **389**, 967 (2008).
- [31] S. Deb, D. M. Goldberg, and V. J. Ramdass, The Astrophysical Journal **687**, 39 (2008).
- [32] D. Coe, N. Ben, T. Broadhurst, and L. A. Moustakas, The Astrophysical Journal **722**, 1 (2010).
- [33] K. Umetsu, T. Broadhurst, A. Zitrin, E. Medezinski, and L.-y. Hsu, The Astrophysical Journal **729**, 127 (2011).
- [34] J. Merten, D. Coe, R. Dupke, R. Massey, A. Zitrin, E. S. Cypriano, N. Okabe, B. Frye, F. G. Braglia, Y. Jimenez-Teja, N. Benitez, T. Broadhurst, J. Rhodes, M. Meneghetti, L. A. Moustakas, L. Sodre Jr., J. Krick, and J. N. Bregman, Monthly Notices of the Royal Astronomical Society **417**, 333 (2011), arXiv:arXiv:1103.2772v3.
- [35] B. Ragozzine, D. Clowe, M. Markevitch, A. H. Gonzalez, and M. Bradač, The Astrophysical Journal **744**, 94 (2012).
- [36] J. Kneib, J. Richard, A. Morandi, M. Limousin, and E. Jullo, arXiv:1209.0384 (2012), arXiv:arXiv:1209.0384v1.
- [37] M. J. Jee, A. Mahdavi, H. Hoekstra, A. Babul, J. J. Dalcanton, P. Carroll, and P. Capak, The Astrophysical Journal **747**, 96 (2012).
- [38] D. Clowe, M. Markevitch, M. Bradač, A. H. Gonzalez, S. M. Chung, R. Massey, and D. Zaritsky, The Astrophysical Journal **758**, 128 (2012).
- [39] C. Lage and G. Farrar, arXiv: astro-ph/1312.0959 (2013), arXiv:arXiv:1312.0959v1.
- [40] D. Harvey, R. Massey, T. Kitching, A. Taylor, and E. Tittley, arXiv:1503.0767 (2015).
- [41] D. Sijacki and V. Springel, Monthly Notices of the Royal Astronomical Society **366**, 397 (2006), arXiv:0509506 [arXiv:astro-ph].
- [42] G. W. Angus and S. S. Mcgaugh, Monthly Notices of the Royal Astronomical Society **383**, 417 (2008).